

A methodology to liberate critical metals in waste solar panel

Li, Mingkai; Widijatmoko, Samuel D.; Wang, Zheng; Hall, Philip

DOI:

[10.1016/j.apenergy.2023.120900](https://doi.org/10.1016/j.apenergy.2023.120900)

License:

Creative Commons: Attribution (CC BY)

Document Version

Publisher's PDF, also known as Version of record

Citation for published version (Harvard):

Li, M, Widijatmoko, SD, Wang, Z & Hall, P 2023, 'A methodology to liberate critical metals in waste solar panel', *Applied Energy*, vol. 337, 120900. <https://doi.org/10.1016/j.apenergy.2023.120900>

[Link to publication on Research at Birmingham portal](#)

General rights

Unless a licence is specified above, all rights (including copyright and moral rights) in this document are retained by the authors and/or the copyright holders. The express permission of the copyright holder must be obtained for any use of this material other than for purposes permitted by law.

- Users may freely distribute the URL that is used to identify this publication.
- Users may download and/or print one copy of the publication from the University of Birmingham research portal for the purpose of private study or non-commercial research.
- User may use extracts from the document in line with the concept of 'fair dealing' under the Copyright, Designs and Patents Act 1988 (?)
- Users may not further distribute the material nor use it for the purposes of commercial gain.

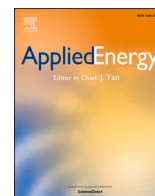
Where a licence is displayed above, please note the terms and conditions of the licence govern your use of this document.

When citing, please reference the published version.

Take down policy

While the University of Birmingham exercises care and attention in making items available there are rare occasions when an item has been uploaded in error or has been deemed to be commercially or otherwise sensitive.

If you believe that this is the case for this document, please contact UBIRA@lists.bham.ac.uk providing details and we will remove access to the work immediately and investigate.



A methodology to liberate critical metals in waste solar panel

Mingkai Li^a, Samuel D. Widijatmoko^b, Zheng Wang^{a,c}, Philip Hall^{a,c,*}

^a Department of Chemical and Environmental Engineering, University of Nottingham Ningbo, China

^b School of Chemistry, University of Nottingham, United Kingdom

^c Nottingham Ningbo China Beacons of Excellence Research and Innovation Institute, Ningbo 315100, China

ARTICLE INFO

Keywords:

Recycling
Solar panel
Critical metal
Selective liberation

ABSTRACT

The availability of critical metals is one of the driving factor to secure the transition of energy production to a renewable, low carbon one because of the material requirement in photovoltaic technology (PV), wind power generation and batteries. For example, precious metals are vital to manufacture crystalline silicon solar panel and tellurium, germanium, indium and gallium are essential in thin film photovoltaic panels. However, the pressure on the supply of critical metals increases with the growth of photovoltaics. Considering the resource availability, the recycling of critical metals from waste solar panels can enhance the sustainability of end-of-life management, although the recycled metal input is limited in present state. Among the recycling techniques, the separation and liberation of metals from non-metals are crucial. This study investigate a methodology to liberate thin film materials from copper indium gallium selenide (CIGS) thin-film solar panel to recycle photovoltaic material including indium and gallium via a mechanical process.

An experimental technique using mineral processing techniques, crushing and grinding, are proposed to recycle critical metals from CIGS solar panel. In this study, the crushing experiments were conducted and the size based elemental distribution was analysed. The results showed crushing is capable to delaminate glass substrate and Fuerstenau upgrading curves and the ore separation degree were used to show that selective liberation occurs and the critical metals concentrate in coarse size fraction but may not be fully liberated. The morphology test using SEM-EDS to observe the surface of broken panel and the classification of broken particle based on size, metal concentration and surface morphology were conducted. The results suggested that approximately 90 w% of functional materials are still laminated on EVA in the size fraction larger greater than 2360 μm . It shows crushing alone will not fully liberate the material. Grinding can be used as a second stage recycling method, de-coating the target materials. The grinding test resulted in a more than 80 w% recovery rate of indium and the fine particle less than 38 μm contains more than 1500 ppm indium, more than 480 ppm gallium and 1500 ppm molybdenum. It could show that the combination of crushing and grinding is suitable to delaminate the panel and de-coat the critical metals to liberate and concentrate the metals.

1. Introduction

As the world moves away from fossil fuels, the renewable energy provides a pathway towards carbon neutrality in the global energy sector as the transition to reduce climate change and adapt to a green economy [1]. Energy efficiency and renewable energy sources relies on technologies and these technologies are often dependent on the supply of raw materials especially metals [2]. These metals are called critical metals, in terms of supply risk and economic importance. Critical metals dominate the performance of energy storage, such as batteries and hydrogen storages, and renewable energy generation including solar

electricity, wind power and fuel cells [2].

Renewable electricity generation was expanding in the past decade and reached the highest share recorded in 2020, as 29 % of the global electricity generation [3]. Photovoltaic (PV) technology, which converts solar radiation into electricity, has been considered to contribute to the transition of the energy structure from fossil fuel dominance to renewables; since solar itself is safe, reliable, efficient, non-polluting and widely distributed [4]. PV has been used since the 1990 s [5] and become one of the major renewable energy sources around the world [6]. The newly installed PV capacity worldwide has been increasing rapidly since 2006 [7]. The total PV capacity reached 586,872

* Corresponding author.

E-mail address: Philip.Hall@nottingham.edu.cn (P. Hall).

<https://doi.org/10.1016/j.apenergy.2023.120900>

Received 12 August 2022; Received in revised form 10 February 2023; Accepted 22 February 2023

Available online 4 March 2023

0306-2619/© 2023 The Authors. Published by Elsevier Ltd. This is an open access article under the CC BY license (<http://creativecommons.org/licenses/by/4.0/>).

megawatts in 2019 and raise to more than 707,000 megawatts in 2020 [8,9]. It is believed the market share of PV power in primary global energy sources will keep expanding in the next decades. It was predicted that cumulative PV capacity will reach 4,000 GW in 2050 [10]. The large scale of photovoltaics will build up more pressure on the cost, resource availability and environmental impact [11]. PV panel manufacturers provide a warranty of between 25 and 30 years [12] and there will be a challenge to recycle a large amount of decommissioned PV modules [13], which is estimated to be approximately 60 million tonnes of panels by 2050 [10]. However, China, the United States and Japan, are the leading markets in solar panels. None of these countries have issued legislation in terms of the disposal of wasted panels [14].

On the basis of power generation unit, solar panels can be classified into three distinguished groups which are first-generation crystalline silicon solar cells, second-generation thin-film solar cells, and third-generation novel cells. The majority of materials in crystalline silicon solar cells is silicon but silver are used as metal strips and thin film panels comprise more critical metals including tellurium, germanium, indium and gallium [2], as well as some important metals such as molybdenum and zinc. Copper indium gallium selenide (CIGS) is a type of photovoltaic material in second-generation thin-film solar panels. It is believed that CIGS panels are promising PV panels with the energy conversion efficiency of the commercial product reported at 15 % [15] and the highest reported lab-scale efficiency of 22.6 % [16].

Fig. 1 illustrates the lamination of CIGS solar panel [17]. CIGS solar cells are made up of a few microns thick CIGS absorber layer, 50–80 nm thick CdS window layer, 50 nm thick ZnO buffer layer, an 0.5–1.5 μm thick transparent conductive oxide (TCO), top contact grid in sequences on glass with a 500–1000 nm thickness molybdenum (Mo) coating as back contact and covered by front glass substrate with Ethylene-vinyl acetate (EVA) [17,18]. In this study, these layers excluding Mo are summarised as functional layers and molybdenum is regarded as back contact layer. The photovoltaic capacity in thin-film solar panels is provided by absorber layer materials comprising indium and gallium, which are viewed as critical raw materials by European Union [19]. There are 45 g indium, 14 g gallium and 230 g molybdenum in 1 kg CIGS solar panel. The concentration is higher than its raw ore, for example, the concentration of indium in raw ore is 10–20 ppm, [20] The reserves of these critical metals are limited and will be run out in 5–50 years [21]. For example, the reserve of indium is only 15,000 tonnes but the mining is likely to be concentrated over the next several decade [22]. The price

of indium in 2021 was \$187 per kilogram in January and raised to \$270 per kilogram in October [23]. These critical metals provide economic incentives to recycle this type of PV device. Whereas the economic benefit for the recycling of other types of panels is outweighed by other means of disposal such as landfilling [24]. In addition, the waste CIGS panels have cancerogenic and ecotoxicity potential due to metals contained [25]. Thus, CIGS modules should be recycled from both resource conservation and reducing environmental pollution perspectives. Currently, the secondary resources can buffer the demand shocks but in long term, it can not affect the demand from primary mining [22], thus a proper recycling method should be developed.

Investigation into the recycling of CIGS PV panels has been reported since the 1990 s. The general procedure can be divided into three stages:

- the delamination of PV modules
- de-coating of the substrate, and extraction
- refining of materials [26].

In the first stage, the laminated modules are shattered using mechanical separation, thermal processes, surface chemistry, solvent processes, cryogenic process, or leaching. Then the de-coating stage aims to remove mass cover glass and EVA binder using dry mechanical method [27], chemical method [28], or the combined method. The further extraction process aims to achieve the purity required for photovoltaic material production. The possible solution includes precipitation, liquid–liquid extraction, electro-winning, ion-exchange, redox process, and etc. [26]. Mineral processing techniques are primarily employed as a pre-treatment process in material recycling to minimise the energy and chemical consumption for the subsequent chemical processes. Crushing can be a common and practical method for pre-treatment [29], it functions to reduce the size and partially liberate materials, however, the effect on liberation varies from samples and crushing techniques. To improve the efficiency of the final stage refinery and save the chemical and energy consumption, a recycling process to liberate and concentrate critical metals using mineral processing techniques are developed.

Solar panel are similar to most minerals that are finely disseminated and associate with the non-target materials, regarded as the gangue. Mineral processing techniques aim to ‘unlocked’ or ‘liberated’ before the separation can be undertaken [30]. In the case of thin film solar panel recycling, the purposes of mineral processing techniques are to reduce the size of waste panel for further treatment, and also expose the target

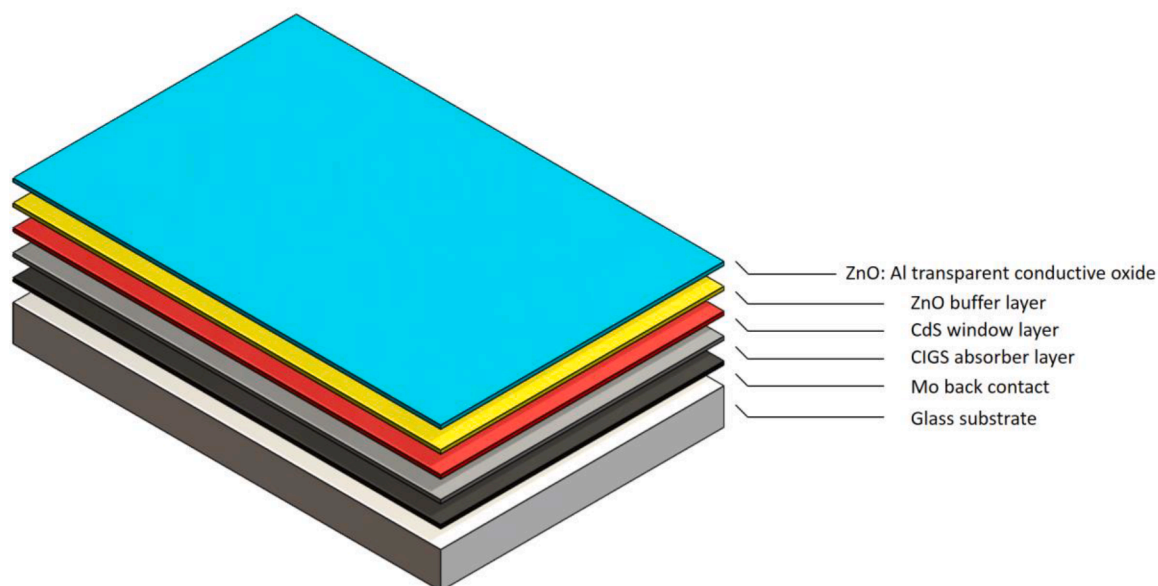


Fig. 1. Cross-sectional views of CIGS thin-film solar cell, adapted from Miles, R.W., G. Zoppi, and I. Forbes.

materials from cover glass or liberate them into certain size fraction [28,31–33], but not to concentrate the metals to the next order of magnitude. Based on the thin film structure of CIGS solar panel, grinding with grinding media can possibly liberate and concentrate the critical metals from dozens ppm to even 1000 ppm. It can be regarded as an efficient and cheap way to de-coat the metals and pre-purify the non-leachable materials before the refinery and extraction. Crushing is proposed as the delamination of CIGS solar panel and to investigate the feasibility of the implementation of grinding technique to de-coat critical metals, the characteristics of crushed CIGS solar panel are studied in this paper.

In ore comminution, the propensity is to concentrate some metals into specific size fractions [34] and the selective liberation phenomenon has also been found in electronic waste [29,35]. In the mineral processing and recycling selective liberation is commonly used as an energy saving technique to concentrate the target materials. However, the outcomes of selective liberation vary from samples and a general summarisation is not suitable to understand the occurrence of that in different sample or comminution process [36]. Whether the valuable materials in CIGS solar panels are liberated during initial comminution has not been studied. Therefore, this study aims to understand the characterisation of milled CIGS solar panels and investigate the liberation behaviour of functional materials. The metal contents from thin-films and molybdenum coating are regarded as valuable material to be recycled and the phenomenon of selective liberation among functional material, molybdenum coating and glass substrate is explored as well. Eventually, a trial of grinding as the de-coating process was tested.

- This paper shows a feasible experimental technique for recovering critical resources, particularly CIGS. This paper aims to develop a recycling process using mineral processing techniques, which is the combination of crushing and grinding to liberate the target material. The major contributions are, Examine the feasibility of crushing as the first stage recycling method,
- Investigate the selective liberation of the critical metals after milling,
- Investigate a suitable solution based on mineral processing techniques to liberate and concentrate the critical metals as the second stage recycling method.

2. Experimental PROCESS

2.1. Materials

Off the shelf products manufactured by Solibro GmbH company, Germany in year 2015 and has not been used but stored were used in this study. These Solibro SL2 CIGS thin-film modules have been tested and certified for IEC 61646/61730, UL 1703 (CSA). The front cover of the panel is 4 mm tempered low iron glass with anti-reflective coating and the back cover is 3 mm float glass. The dimension of the panel is 1190 (+3/-1) mm length, 789.5 (+3/-1) mm width and 7.3 mm thick without junction box. The junction box has a dimension of 66 mm length, 54 mm width and 14.5 mm thick with 1 bypass diode. Solar cable attached with junction box has a cross-sectional area 2.5 mm² and tip and ring with 855 (+30/-0) mm and 735 (+30/-0) mm respectively.

The elements in the absorber layer, buffer layer, window layer and back contact layer were confirmed as indium, gallium, molybdenum, copper, aluminium, zinc and cadmium, using Scanning Electron Microscopy-Energy Dispersive X-ray (SEM-EDX, Zeiss – Oxford/ Sigma VP). In addition, the metal wire between the front cover and back substrate glass at the edge was confirmed as aluminium. In this study, functional materials are represented by characteristic metal elements contained in different functional layers, which is indium representing CIGS absorber layer, zinc representing buffer layer, Cd representing window layer and molybdenum representing back contact layer. The binder was identified using Fourier-transform infrared spectroscopy (FTIR, Bruker- VERTEX 70) and found to be Ethylene-vinyl acetate

(EVA). HNO₃, HCl, and H₂O₂ (PURISS-PA grade, Sigma-Aldrich) and water (specified as grade 1 in ISO 3696) were used during digestion and dilution for elemental analysis.

2.2. Experimental method

The experiment started with the crushing of CIGS solar panel and a size characterisation was conducted to analyse the distribution of crushed sample. After that, elemental analysis was employed to investigate the liberation of critical metals and the occurrence of selective liberation. The following morphology analysis aims to observe the liberated thin film structure and help determine the next stage recycling method. The classified categories were summarised then. Finally, a trial of grinding test was conducted and the results were analysed.

The overall framework of proposed experimental method is shown as Fig. 2. The plastic junction box and cables of CIGS solar panel sample were separated first (Fig. 2 (b)) and the panel was hammered manually (Fig. 2 (a)). All fragments were collected and the mass loss due to breaking is less than 0.1 wt%. The smashed solar panel was milled using Restch SM 2000 cutting mill with an 8 mm grid. The milled sample was dried in an oven at 105 °C to remove moisture content; adapted from BS 812–109:1990 [37] and the mass change is less than 0.1 w %.

The milled panel weighed approximately 16.2 kg and 32 representative samples were then obtained using a static riffle. Three representative samples of average weight 501.3 g were sieved using certified Endecotts test sieves and a Capco Inclino Sieve Shaker 3 Sieves. Sieves with aperture size range from 38 µm to 13200 µm were used initially and sieves with nominal aperture diameter of 13200 µm, 4750 µm, 3350 µm, 2360 µm, 1180 µm, 600 µm, 300 µm, 150 µm and 75 µm were selected. All size fractions were used and these sieve sizes were selected to present the distribution because the curve generated is the same as original one but can minimise the sieve number used. Then elemental analysis with ICP-MS was conducted for each size fraction.

To conduct the elemental analysis by ICP-MS, the composition of interest in samples need to be extracted into solution via digestion. To ensure leaching efficiency in digestion, the size of particles should be controlled to be less than 250 µm, thus further size reduction is required for size fractions larger than 250 µm. Particles size fraction larger than 1180 µm contains EVA binder and is difficult to be milled therefore EVA is removed first. These fractions were transferred to porcelain lidded crucibles and calcined in a muffle furnace. Multistage calcination was used to remove EVA. The temperature was ramped to 250 °C with a temperature rate set as 10 °C/minute and held for 1 h. Then the temperature was raised to 400 °C, with a rate of 15 °C/minute, holding for 1 h, the same rate was set again to 500 °C with 2 h holding time [38].

Size fractions larger 200 µm than were milled using Retsch ZM 200 centrifugal mill with 0.25 mm grid. Particles inside and outside the grid were carefully collected and sieved with 212 µm nominal aperture size. The particle fraction larger than 212 µm was re-milled and sieved until the recovery rate is more than 95 wt%.

The samples were prepared using microwave-aided acid digestion with CEM MARS 5 microwave digester. The digestion method was adapted from BS EN 62321–5:2014 [39]. 200 ± 0.1 mg sample was weighed using an analytical balance to four decimal places. The microwave digester operating programme is shown in Table 1. In the first stage the sample was placed into a digestion vessel, 4 ml of 65 wt% HNO₃, 1 ml of 50 wt% H₂O₂, and 1 ml of water (Grade 1 in ISO 3696) were then added. In the second stage, 4 ml 37 wt% HCl was added into each vessel.

The elemental analysis was conducted via PerkinElmer-NexION® 300x Inductively Coupled Plasma-Mass Spectrometer (ICP-MS). To investigate the liberation of functional materials from buffer layer, window layer, absorber layer, and back contact layer, the concentrations of indium, gallium, molybdenum, copper, aluminium, zinc and cadmium were measured. A set of mixed matrix standard solutions was prepared from certified reference materials in accordance with ISO/IEC

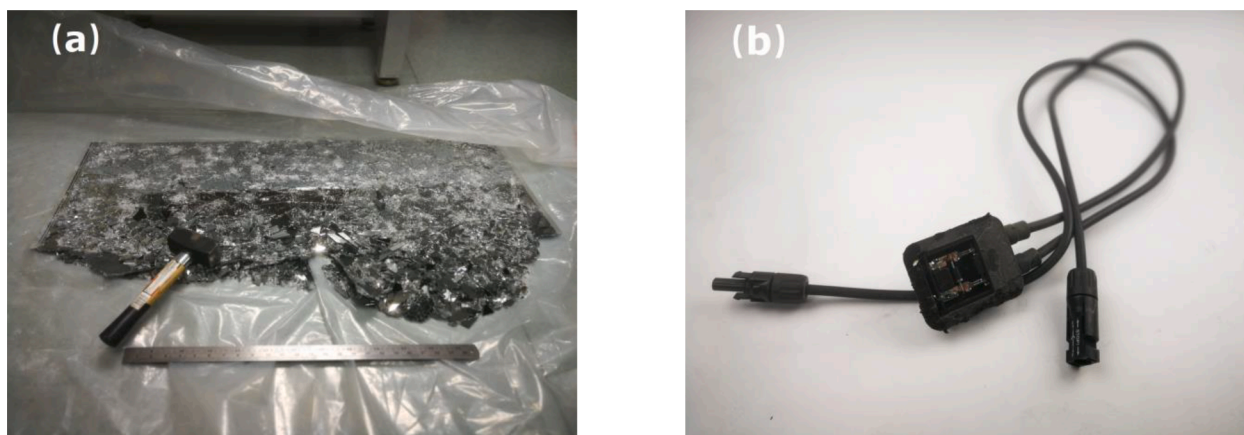


Fig. 2. The overall framework of proposed method.

Table 1
Microwave digestion method.

Stage	Number of digestion vessel	Power (W)	Ramping time (min)	Temperature (°C)	Hold time (min)
1	10	1600	8	80	10
	10	1600	8	160	20
Cooling	10	1600	8	less than 30	10
	10	1600	8	160	20

17,025 and ISO 17034 (ISO Guide 34).

Morphology study was carried out using a Zeiss FESEM with Oxford/Sigma VP EDS detector to observe the surface of broken particle. Samples were prepared by coating 10 nm gold layer with LEICA EM SCD 500 gold sputtering machine to ensure surface conductivity for high-resolution imaging.

After the characterisation, a trial of grinding was conducted via attrition scrubbing. The feasibility of attrition scrubbing to liberate CIGS material is investigated by analysing a 5 min attrition scrubbing with 70 wt% pulp density. After the end of attrition scrubbing, the attrition product was sieved into size fractions greater than 4350 μm, 4350 μm–3350 μm, 1180 μm–3350 μm, 150 μm–1180 μm, 38 μm–150 μm, and less than 38 μm, and the sieved attrition product fractions were analysed. Low ion silicon sand with size fraction 1180 μm–2360 μm was used as attrition media. The ratio of attrition media to sample is set as 2:5 by weight.

3. Results and discussion

3.1. Concentration distribution of milled CIGS solar panel

499.8 g CIGS solar panel sample was milled using cutting mill and sieved into size fractions as described previously. The characterization of CIGS panels started with analysing the significance of weight distribution [40]. Weights of sieved products were measured and cumulative undersize was used in this study to assess the particle size distribution of grinded CIGS solar panel sample, shown in Fig. 3. Fig. 3 (a) illustrates the weight of different size fractions and the weight increases with size and reaches the peak at the size fraction 2360–3350 μm than drops. More than 300 g of particles distribute in the size fraction 1180–4750 μm. Fig. 3 (b) illustrates the accumulated undersize weight among all size fraction and the average particle size (d50) is found as approximately 2680 μm. It can also be found that 80 wt% particles after milling were in the coarsest size larger than 1180 μm. Overall, the size distribution reports that majority sample concentrate in the coarse size fraction after milling.

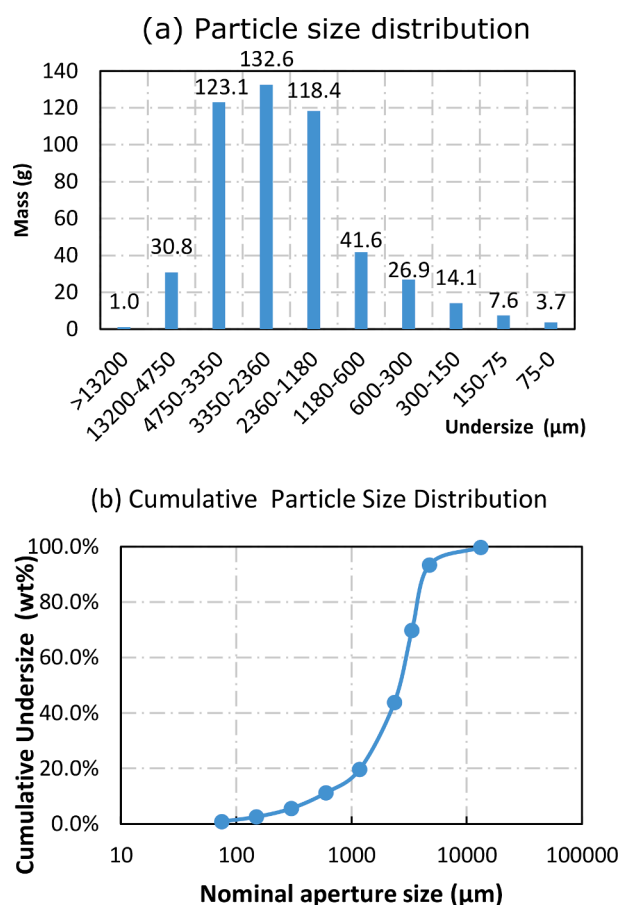


Fig. 3. Particle Size Distribution of milled CIGS solar panel.

Critical metals indium, gallium and other important metals molybdenum, zinc, copper, and cadmium, as well as aluminum, in the solar panel sample have been analysed using ICP-MS, the average results are summarised in Fig. 4 and Fig. 5. The concentration of these metals are not in the same magnitude but the similar distribution patterns shown from Fig. 4 (f) were suggested for five elements, which are In, Ga, Cu, Cd, and Zn, originates from buffer layer, window layer and absorber layers. The most concentrated size fraction of these five metals shown from Fig. 4 (a)–(e) is size fraction 4750–13200 μm and the minimum concentration of In, Ga, Cu and Cd lie in the size fraction 600–1180 μm. For the other two metals analysed, Al and Mo, the concentration illustrated from Fig. 5 increase as particle size decrease, with maximum

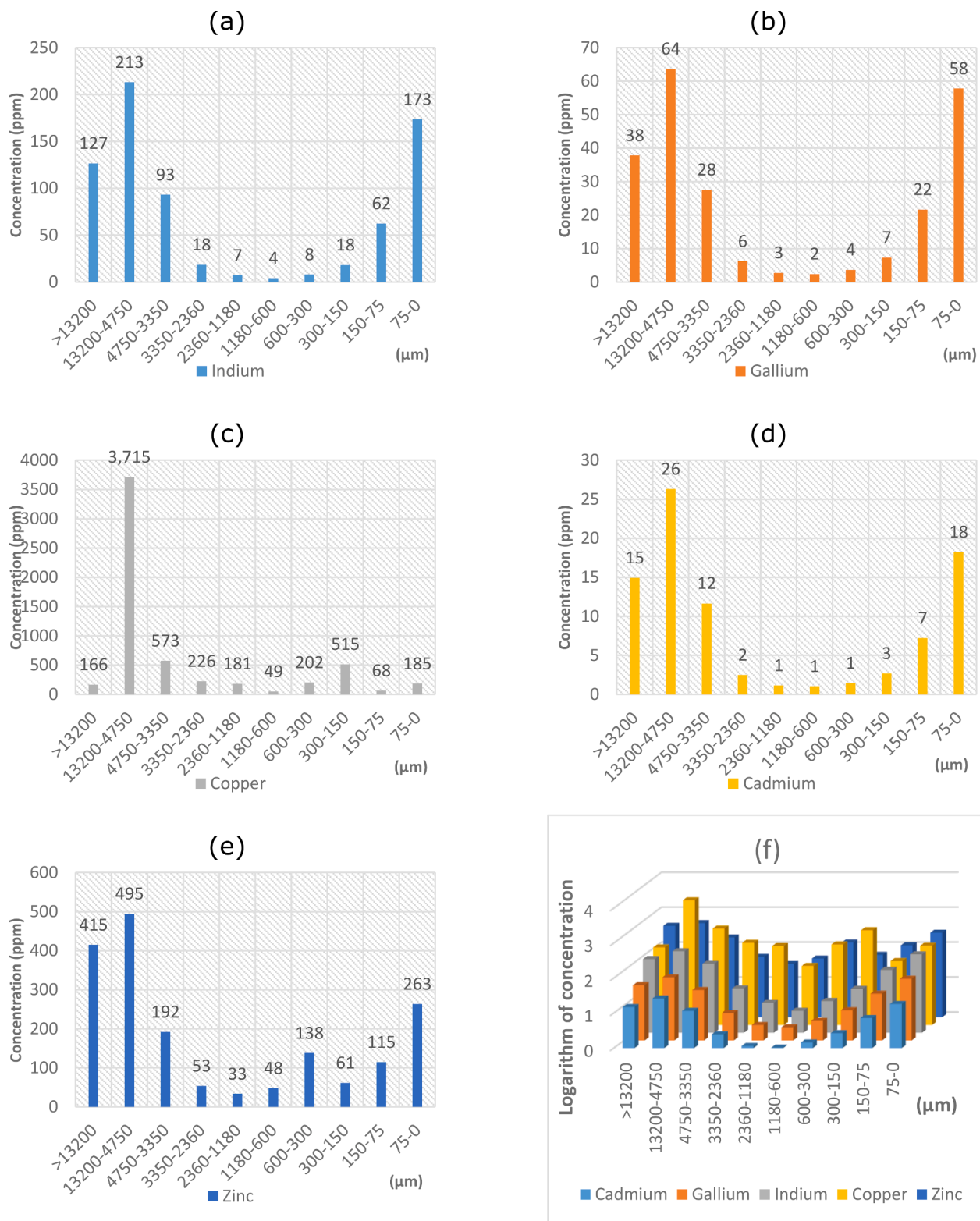


Fig. 4. Size-Concentration Distribution of five elements.

concentration at the size fraction less than 75 μm . Based on the data obtained, metals after milling do not distribute evenly but concentrate in certain size fraction. Considering the mass distribution of sieved product, the selective liberation is to be investigated.

The recovery rate of metals and ore separation degree are calculated to investigate the degree of selective liberation induced by size reduction via cutting mill. The recovery rate (R) of metal is defined as the

weight fraction of metals in this size fraction out of all size fractions, expressed as,

$$R = \frac{m_i}{m} \times 100\%$$

Where m_i = the mass of metal in the i^{th} size fraction (g); m = overall mass of metal (g).

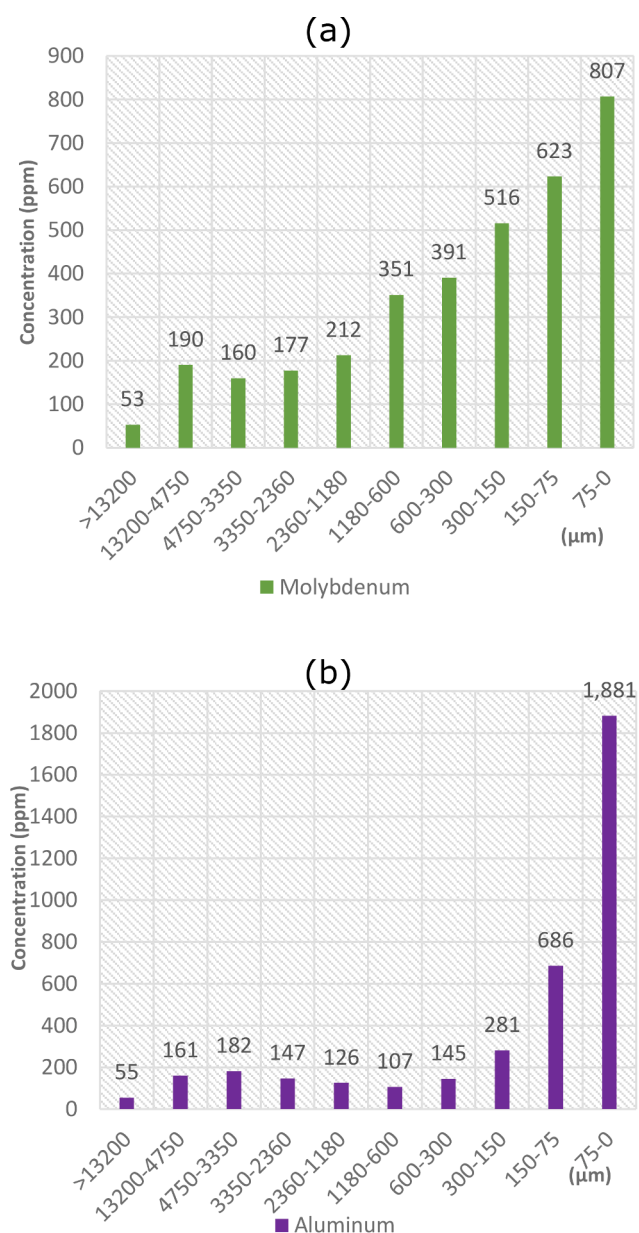


Fig. 5. Size-Concentration Distribution of molybdenum and aluminium.

The liberation of certain material can be represented by ore separation degree (η_{ore}) which is the difference between the recovery rate of valuable material and waste material. The recovery rate varies among particles size and then the particle size is regarded as separation cut point t_d for η_{ore} . it can be expressed as below,

$$\eta_{\text{ore}} = R_v - R_w$$

Where R_v = recovery rate of valuable material, R_w = recovery rate of waste material.

The cutting mill provides shearing and cutting stress to reduce particle size [41]. To investigate the cutting induced selective liberation of functional layer materials in CIGS thin-film solar panel and the interaction of functional thin-film layer materials between the substrate and back contact layer, Fuerstenau upgrading diagram and ore separation degree were plotted.

The Fuerstenau upgrading diagram in recovery plots were used in evaluating selective comminution in the field of mineral processing [42–44] and more recently used in electronic waste recycling [29]. The

recovery of valuable mineral and the waste material for various separation cut points t_d (μm) can be plotted in the diagram and Fig. 6 is an example. The horizontal axis is the accumulated recovery rate with the increase of separation cut point, from the smallest to the largest, and the vertical axis presents the recovery rate of valuable material at the same separation cut point, thus, the advantage of this method is to visually present whether the valuable materials are selectively liberated, or concentrated in a certain size fraction. The diagonal line, line 2 in Fig. 6, illustrates that selective liberation does not occur in the investigated materials. The curve above the diagonal line, line 1 in Fig. 6, documents that valuable material enriches in fine fractions and the curve below the diagonal line, line 3 in Fig. 6, documents an enrichment of valuable material in coarse fraction. In this study, the recovery of valuable material (R_v) and waste material (R_w) is plotted in Fuerstenau upgrading curve as R_v - R_w .

3.2. Selective liberation of metals

In this study, critical metals are regarded as target material and glass is regarded as waste material. Although glass is regarded as waste material in this study, it can be recycled after the removal and recovery of metal contents in a practical process. The selective liberation among absorber layer, buffer layer and window layer was investigated first. Based the Fuerstenau upgrading curve shown in Fig. 7, there was no selective liberation identified. The In-Ga curve in Fig. 7 is close to the diagonal line, which could be explained by the material distribution in the thin-film structure of solar panels. Indium and gallium are from CIGS photovoltaic material and there is no other source of these two elements in solar panel sample, the recovery of gallium was the same, which the condition of copper is the same. Thus, the recovery of indium is used to evaluate the liberation of CIGS absorber layer, and copper and gallium are not mentioned below. Zinc and cadmium are used in buffer layer and window layer respectively. The In-Zinc and In-Cd curves are also close to the diagonal line and that means the materials from buffer layer and window layer are not liberated from the absorber layer, thus the hypothesis is that; after milling, the lamination structure of buffer layer, window layer and absorber layer structure has not been destroyed and making these functional materials stick on each other.

Ore separation degree is the difference between the recovery rate of valuable material and waste material and thus, the sign of η_{ore} indicates the preference of material liberated. In other words, ore separation degree η_{ore} can also evaluate selective liberation [43]. The largest absolute

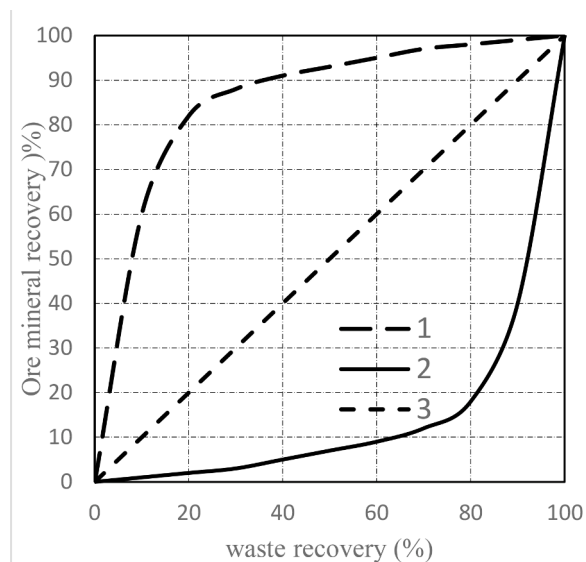


Fig. 6. An example of Fuerstenau upgrading recovery plot adopted from Hesse, M., O. Popov, and H. Lieberwirth.

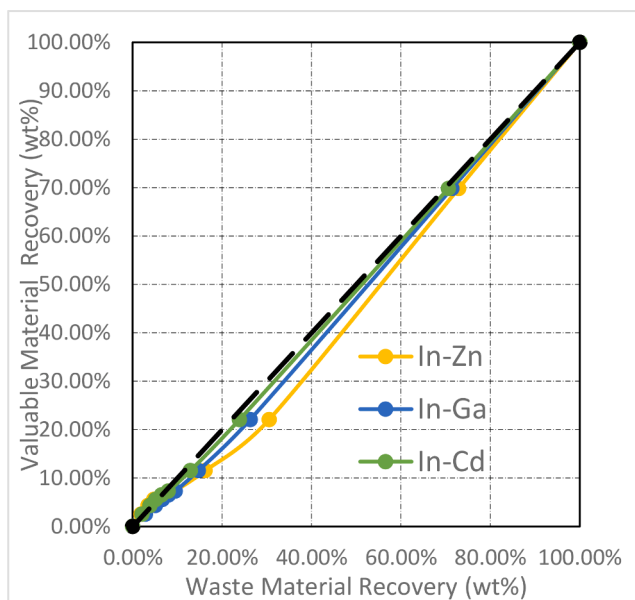


Fig. 7. Fuerstenau upgrading curve of functional material.

number of ore separation degree could indicate the cut point that maximises the recovery of valuable material while minimising the recovery of waste material and the sign indicates which material is preferred to be recovered.

In Fig. 8, the maximum absolute value of ore separation degrees for In-Ga ($|\eta_{ore,In-Ga,max}|$) is 4.19 %. However, indium and gallium can only be found in a same compound which is copper-indium-gallium selenide, it is considered as the error from elemental analysis. Meanwhile, ($|\eta_{ore,In-Cd,max}|$) = 1.80 % and ($|\eta_{ore,In-Zn,max}|$) = 8.42 %. The negative signs show that compared with indium, the other metals are preferred to be recovered. However, the values are not significant to show the occurrence of selective liberation. Both the Fuerstenau upgrading curves and ore separation degree indicate that recovery of functional materials tends to be the same. Hence, milling does not induce selective liberation within buffer layer, window layer and absorber layer.

Fig. 9 shows that milling can selectively liberate thin-film solar

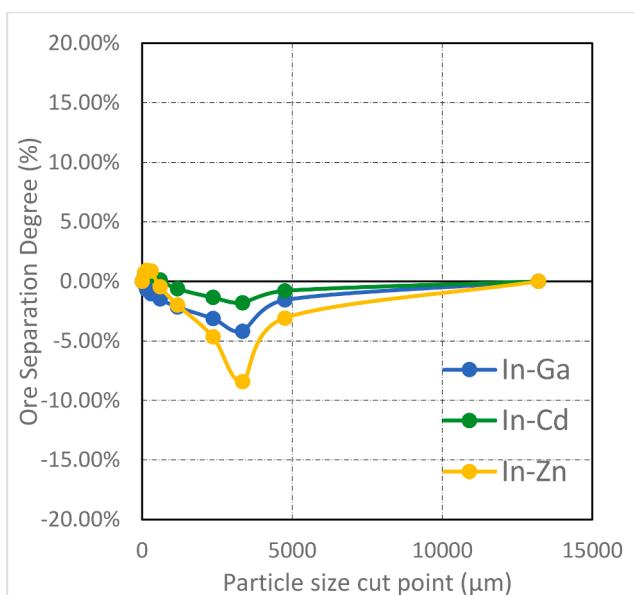


Fig. 8. Ore separation degree curve of functional materials.

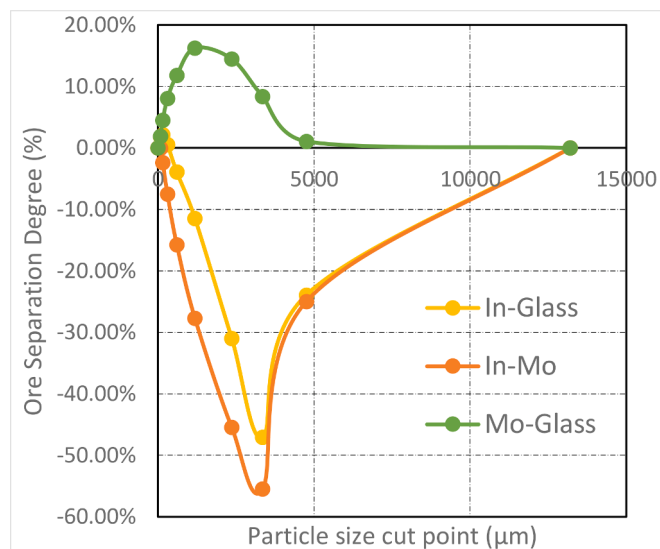


Fig. 9. Fuerstenau upgrading curve of functional material and back coating.

panels by concentrating functional materials from back coating metal and glass substrate. Aluminium was not only found in the thin film structure but also from the metal wires at the edge of the panel, therefore aluminium is not employed to investigate the selective liberation. The recovery of functional material (represented by Indium) is greater than the recovery of glass substrate and back coating metal in the coarser size fraction. The Fuerstenau upgrading diagram can be divided into recovering region before the inflection point and re-mixing region after the inflection point. The In-Mo curve is below the diagonal line, although indium and other functional material are also recovered, the recovery of molybdenum is greater than the recovery of indium in the recovering region and the re-mixing region, the recovery of indium overweighs the recovery of molybdenum. In-Glass curve is different from In-Mo curve since it has two inflection points, the curve is above the diagonal line in the finer size fractions which means the recovery of indium overweighs the recovery of glass, although the difference is not significant. After the first inflection point, cut point of 150 μm , the recovery of indium is slowing down but still greater than the recovery of glass until the curve lies below the diagonal line where the recovery of glass dominates. Furthermore, in the re-mixing region with the cut point greater than 3350 μm , the recovery of indium is increasing. The interaction between molybdenum and glass is also plotted but the Mo-Glass curve performs differently. The recovery of molybdenum increases first by increasing the cut point in the recovering region while accomplishing with the recovery of glass. In the re-mixing region, the increasing cut point yields a higher recovery of Mo but has been outweighed by the increase of glass recovery.

Fig. 10 illustrates the ore separation degree curves of In-Glass, In-Mo and Mo-Glass. Mo-Glass curve shows that among all size fraction, molybdenum is preferred to be liberated compared to glass since the ore separation degree is positive and the cut point 1180 μm yields the maximum ore separation degree where $|\eta_{ore,Mo-Glass,max}|$ is 16.26 % and 65 wt% Mo is recovered below 1180 μm . Ore separation degree of In-Glass is positive, up to 2.14 %, before the cut point 300 μm which means the liberation of indium is slightly preferred. However, the difference is not that significant. The distinguished difference occurs at the cut point 3350 μm , where $|\eta_{ore,In-Glass,max}|=47.1$ %, and the liberation of glass is preferred. In-Mo curve is similar but the ore separation degree at all cut points is negative which means the liberation of molybdenum is always higher than that of indium. The maximum value also occurs at the cut point 3350 μm where $|\eta_{ore,In-Mo,max}|$ is 55.5 %. In the size fraction greater than 3350 μm , the recovery of Indium is 78.9 wt% and the recovery of Molybdenum and glass are 22.5 wt% and 30.8

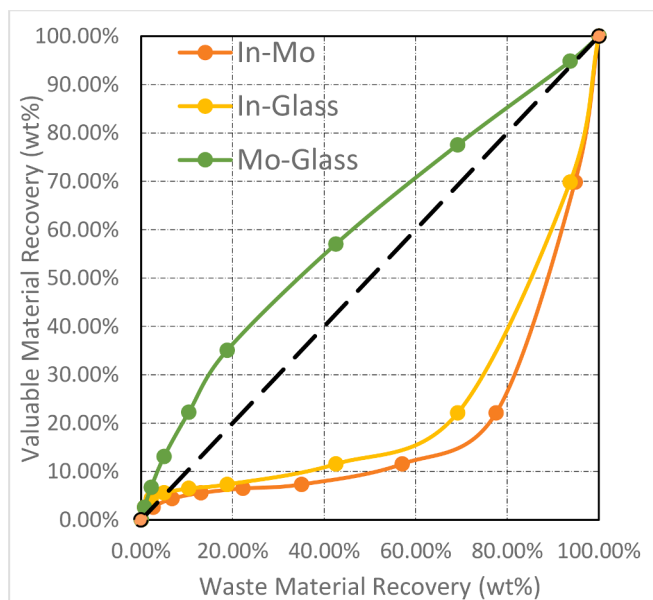


Fig. 10. Ore separation degree curve of functional materials and back coating.

wt%. Overall, the cut point 3350 μm gives the highest efficiency to recover glass and molybdenum while minimising the efficiency to recover functional materials; on the other hand, it is the cut point with the highest potential to recover functional materials and minimum contamination.

From the results presented above, milling alone does induce selective liberation for functional material in thin-film solar panels. Compared to another thin-film material, lithium-ion batteries, whose valuable metal concentrate in fine size fractions [29], functional materials are found to concentrate in coarse size fractions. Furthermore, back contact layer and the glass substrate were selectively liberated from each other. This finding demonstrated variation in the strength of adhesion forces between different constituents in thin-film solar panels, including functional material, EVA, Mo back contact layer, and glass substrate. The cutting stress induced by the cutting mill reduced the size of thin-film solar panels and dislodges the CIGS-Mo interface. It means milling is capable to delaminate glass substrate, however, the effects of comminution on the liberation of functional material from glass substrate cannot be demonstrated by elemental analysis, thus, a morphology analysis using SEM-EDX is carried out.

3.3. Morphology analysis of milled solar panel

The thin film structure of CIGS solar is exposed from the encapsulated glass panels after milling and functional material is visually observed as black films on EVA binder, molybdenum is observed as mirror-like shining particles on the glass substrate and the rest of the particles are glass substrate. EVA is mainly found in the coarse size fraction larger than 2360 μm . The morphology observation aims to observe the surface and analyse the characteristics of the functional layer and molybdenum layer in different size fractions, thus, SEM-EDX is employed. Samples in the size fractions greater than 2360 μm were selected manually to investigate the morphology of EVA attached to the front glass and molybdenum coated on the back substrate. The other size fractions mentioned previously were mounted on the aluminium stage by adhesive carbon tape for morphology study.

Fig. 11 shows the SEM-EDX image of milled samples, the functional materials are either laminated on the EVA binder or liberated into fine particles, and molybdenum are found on the glass substrate. However, SEM-EDX only detected elements from functional materials on glass particles with EVA binder, but not contaminated with molybdenum. It

was discovered that milling can separate functional materials and molybdenum by breaking the front cover glass and the back substrate into different pieces.

For the size fraction greater than 2360 μm , although the detachment of functional materials occurs at the edge where the laminate of functional materials is partially removed, the majority of functional layers are still held firmly with the EVA binder on the glass substrate. The cracks and debris of the functional material layer indicate that milling, as preliminary liberation, induces the breakage of functional layers but still attaching on EVA binder, hence, milling can not liberate the functional materials in size fraction greater than 2360 μm . The molybdenum layer is laminated on the glass surface with no cracks or debris similar to those observed on EVA, which means the preliminary liberation failed to induce the detachment of molybdenum from the glass substrate in the size fraction greater than 2360 μm .

For the size fraction 300–2360 μm , the occurrence of the EVA binder attached to glass is less than that in the coarser size fraction by visual inspection. From Fig. 11 (b), it was inspected that functional materials laminated on the EVA in the size fraction 300–2360 μm but EVA were delaminated from glass, found as fragments. Isolated EVA particles in this size fraction are cut from larger size EVA binder by cutting mill. The detachment of functional materials occurs at the edge where the laminate of functional materials is partially removed, the majority of the functional layer is still held with the EVA binder. The molybdenum layer is still laminated on the glass substrate with no cracks or debris.

For size fraction 75–150 μm , most fine particles observed were clean glass particles without EVA or molybdenum. Fine particles in this size fraction were generated due to the breakage of glass and the liberation of EVA, which also contains some residual functional materials. Fig. 11 (c) demonstrates that in this size fraction, EVA is fully detached from glass and contains some residual functional materials. Functional materials can be found as finer particles less than 10 μm , liberated from EVA binder in the coarser size fraction. Molybdenum is still on the glass surface, however, different from the size fraction greater than 300 μm , where molybdenum is already partially detached.

This surface morphology can illustrate the breakage mechanisms of CIGS solar panels using a cutting mill for preliminary liberation. The delamination of solar panel is achieved and the functional materials with critical metals are exposed but still attached on EVA. The next stage recycling aims to de-coat glass substrate and binder, the resulted liberated particles can be further grinded feasibly to liberate the surface material on EVA and then concentrate the particles in certain size fraction. The concurrence of size-based hierarchy and particle morphology is further discussed to understand the liberation of functional material in solar panels by comminution and help decide the size of media used in the next stage grinding.

3.4. Category of the milled classified CIGS particles

From the size-based hierarchy and the morphological study carried out, the liberated CIGS can be classified into three categories based on the attachment of functional materials on EVA or glass substrate, and the degree of functional materials detachment. The coarse size fractions with functional materials attached to the EVA binder are classified as Category 1 and Category 2 and they are categorised further by the concentration of functional material. The fine size fractions with functional material residual and isolated EVA particles are classified as Category 3. The characteristics of particles in different size fractions are summarised in three catalogues shown in Table 2.

The types of loading of the cutting mill are shearing and cutting stress. The brittle matter is broken into pieces when introduced into the chamber of the cutting mill. The non-brittle materials experience a large deformation while being hit by the edge of the knives, then the cracks begin to grow and propagate until being broken [41]. In the case of milling CIGS solar panel, the cutting stress induced by the cutting mill in this study reduced the size of the glass panel and dislodged the interfaces

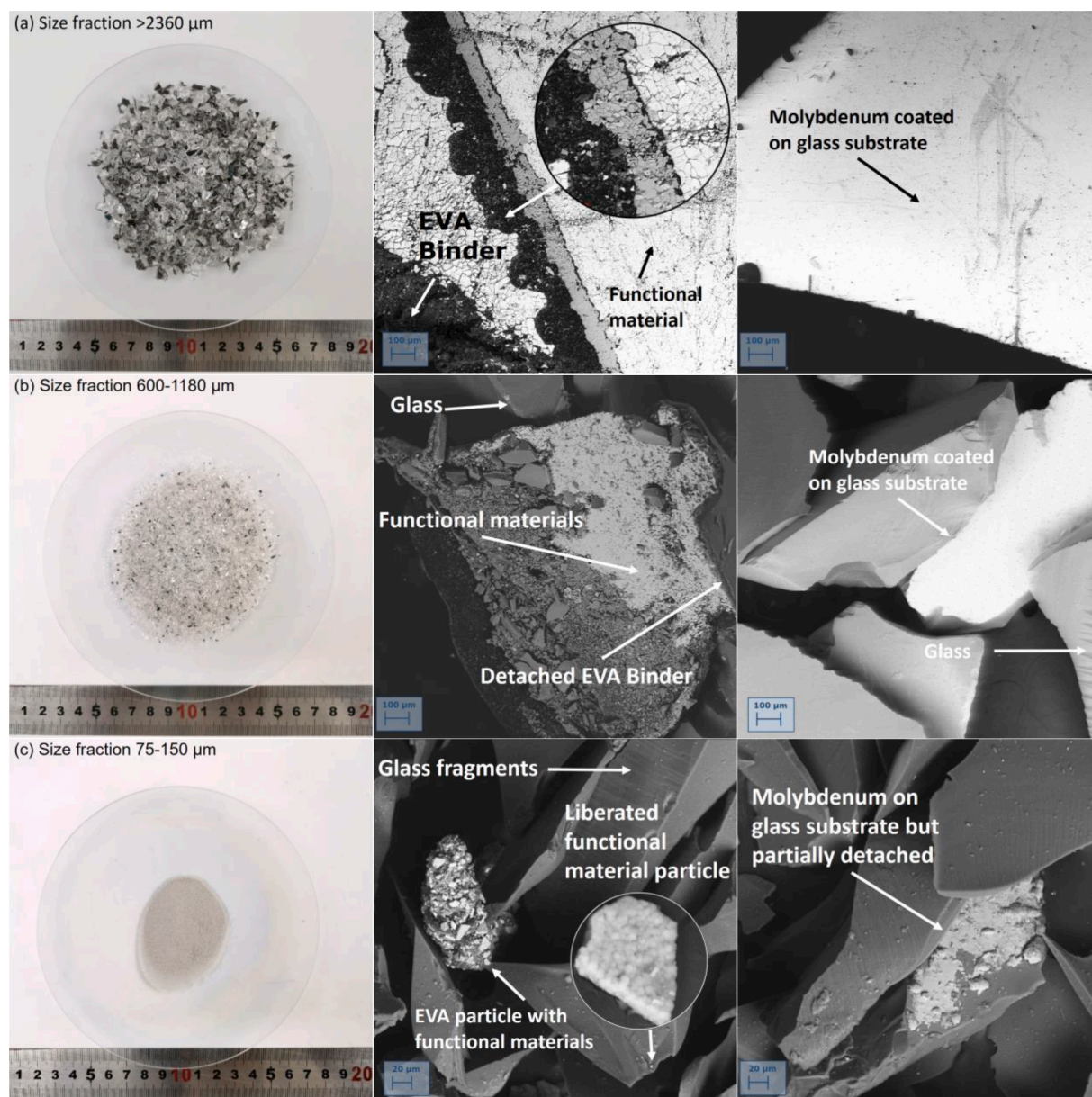


Fig. 11. SEM-EDX image of milled sample.

of compacted thin films, which is the CIGS-Mo interface. The reason is a MoSe₂ layer can form between the Mo and CIGS layers after manufacture [45,46] and also the Na can be leached from the glass substrate [47,48] so that the adhesion between CIGS layer and Mo layer is weaker and easily delaminated while applying a cutting stress.

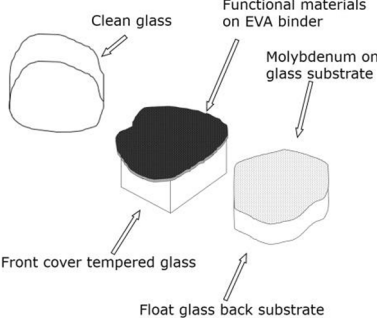
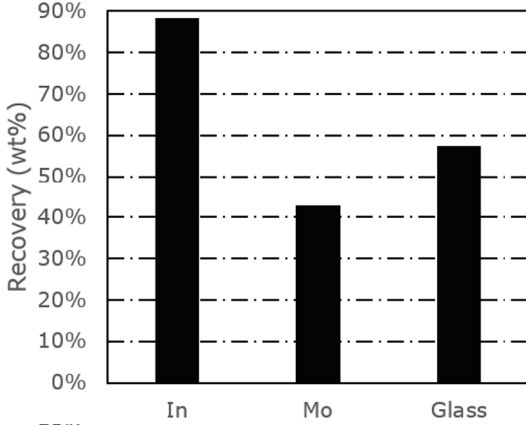
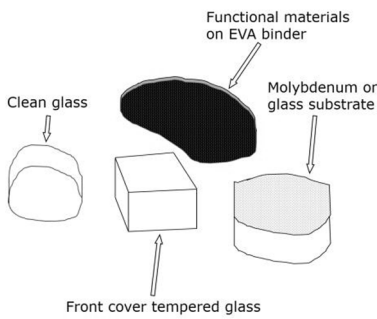
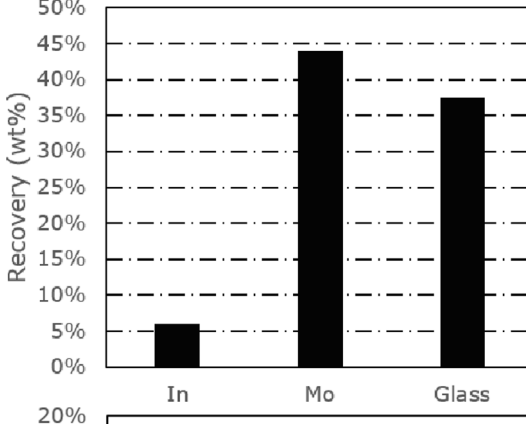
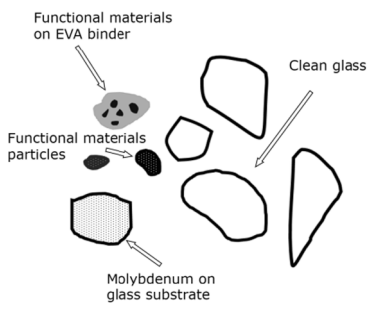
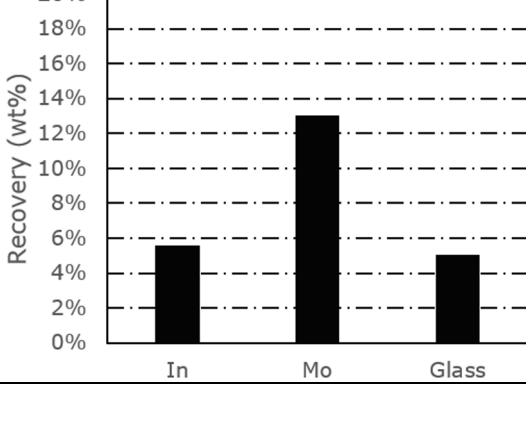
The functions of the front cover and back substrate of the solar panel are different. The back substrate is float glass and it is broken into irregular pieces with the molybdenum layer. The front cover of the CIGS solar panel is tempered low iron glass for its high light transmittance and high strength. If the tempered low iron glass breaks, it will shatter into cubes, through a process called self-explosion. EVA binder attaches on the front cover glass and functional materials remain on the EVA binder because of the breakage of CIGS-Mo interface. Based on the breakage mechanism mentioned above, EVA tends to experience deformation and then break with front cover glass cubes. Moreover, the shearing induced by the cutting mill is not sufficient to delaminate the functional materials out of EVA and instead, functional materials cover almost the whole surface area of the EVA binder. Thus, the broken front cover glass with EVA and functional materials, broken back substrate and some clean

glass particles are classified as Category 1. This category in coarse size fraction greater than 2360 μm, concentrates approximately 89 wt% functional materials and 43 wt% molybdenum. From Fig. 10 and Fig. 9, category 1 leads to the highest potential to recover functional materials.

Category 2 refers to particles in the size fraction 300–2360 μm. EVA binder is torn off the large particles to be isolated from glass, results in a smaller EVA particle free from glass. From Fig. 11 (b) The deformation of EVA reduce the liberation of functional materials only at the edge of isolated EVA particle. However, the amount of liberated EVA particles are not significant, only 6 wt% functional materials are classified in this category. Based on the breakage mechanism, shearing can localise low intensity of surface tension and results in the breakage of particles and polish the surface of the particle [49]. Although the shearing by cutting mill can not liberate functional materials on the EVA binder, it can polish the surface of molybdenum and glass substrate. From Fig. 9 and Fig. 10, molybdenum concentrates in category 2.

Due to the deformation of EVA, breakage of glass, and polishing of particles during milling, size fraction less than 300 μm is classified as category 3. Category 3 contains clean glass, isolated EVA particles,

Table 2
Characterisation of classified CIGS particles.

Schematic diagram	Recovery rate								
<p>Category 1 >2360 μm</p> 	 <table border="1"> <thead> <tr> <th>Element</th> <th>Recovery (wt%)</th> </tr> </thead> <tbody> <tr> <td>In</td> <td>~88</td> </tr> <tr> <td>Mo</td> <td>~42</td> </tr> <tr> <td>Glass</td> <td>~58</td> </tr> </tbody> </table>	Element	Recovery (wt%)	In	~88	Mo	~42	Glass	~58
Element	Recovery (wt%)								
In	~88								
Mo	~42								
Glass	~58								
<p>Category 2 300-2360 μm</p> 	 <table border="1"> <thead> <tr> <th>Element</th> <th>Recovery (wt%)</th> </tr> </thead> <tbody> <tr> <td>In</td> <td>~6</td> </tr> <tr> <td>Mo</td> <td>~44</td> </tr> <tr> <td>Glass</td> <td>~37</td> </tr> </tbody> </table>	Element	Recovery (wt%)	In	~6	Mo	~44	Glass	~37
Element	Recovery (wt%)								
In	~6								
Mo	~44								
Glass	~37								
<p>Category 3 <300 μm</p> 	 <table border="1"> <thead> <tr> <th>Element</th> <th>Recovery (wt%)</th> </tr> </thead> <tbody> <tr> <td>In</td> <td>~5.5</td> </tr> <tr> <td>Mo</td> <td>~13</td> </tr> <tr> <td>Glass</td> <td>~5</td> </tr> </tbody> </table>	Element	Recovery (wt%)	In	~5.5	Mo	~13	Glass	~5
Element	Recovery (wt%)								
In	~5.5								
Mo	~13								
Glass	~5								

liberated functional materials and molybdenum on glass. Although it counts for less than 5 wt% of total sample, the liberated functional materials are mainly within this size fraction.

The results suggested that the majority of functional material with critical metals after milling still laminate on EVA binder, but already exposed. Approximately 90 w% of functional materials are still laminated on EVA in the size fraction larger than 2360 μm and thus, the feasibility of the implementation of grinding to liberate and concentrate the critical metals has been shown. That can also help determine the size of grinding media, which should be less than 2360 μm so that the surface materials can be liberated and minimise the generation of glass particle in the fine size fraction.

3.5. Grinding test

The characterisation of the broken CIGS solar panel, including the

element distribution, morphology test and categories of classified particles, shows the surface polishing can be a proper solution to liberate and concentrate critical metals after the first stage delamination via crushing. Grinding is proposed to de-coat the broken panel as the second stage recycling process to yield concentrated metal contained product for metal refinery and extraction.

The experiment employed attrition scrubbing to test the performance of grinding. A 5 min attrition scrubbing was conducted with 70 w% pulp density and the attrition media was chosen as low ion silicon sand so that the media would not bring contamination for the product. The size of attrition media should be less than 2360 μm based on the study above, thus size fraction 1180 μm -2360 μm was chosen. The results are shown as Fig. 12 and Fig. 13.

Fig. 12 shows that after 5 min attrition scrubbing, 82.64 w% of indium has been concentrated in the size fraction less than 38 μm . Based on Fig. 13, comparing with molybdenum and glass, indium is selectively

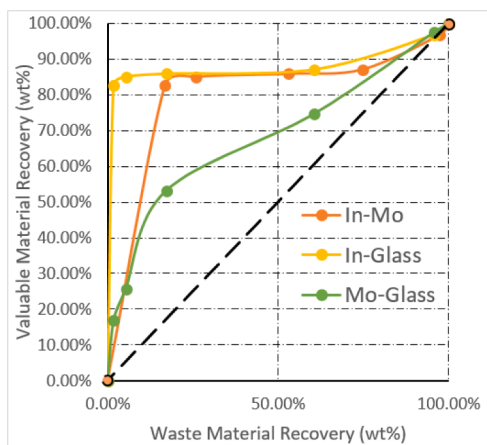


Fig. 12. Fuerstenau upgrading curve of attrition scrubbing trial.

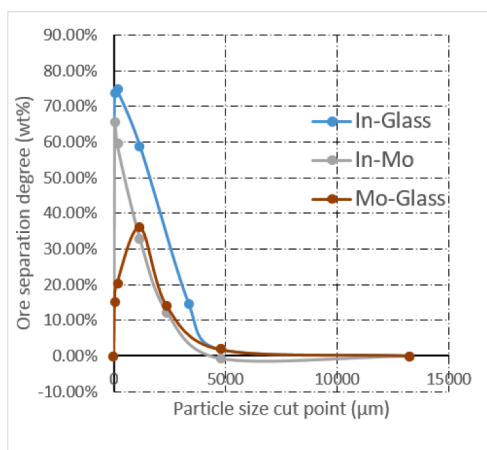


Fig. 13. Ore separation degree curve of attrition scrubbing trial.

liberated. Grinding with media yield 13.7 g fine particles from 500 g sample and 200 g attrition media with 1506 ppm indium 482 ppm gallium and 1589 ppm molybdenum. The results shows that along with crushing as the first stage delamination process, grinding, more specifically, attrition scrubbing.

4. Conclusion

This study presents a systematic study aiming at the investigation of selective liberation of functional materials in CIGS solar panels during milling to examine the feasibility of grinding as a de-coating process to liberate and concentrate the critical metals. The results of experiments demonstrated the phenomenon of selective liberation of materials from buffer layer, window layer and absorber layer with an optimum cut point of 3350 μm . In the size fraction greater than 3350 μm , metals from buffer layer, window layer and absorber layer recovered is more than 70 w%, for example the recovery of CIGS is 78.5 wt% zinc is 70.5 wt In the same size fraction, a 22.5 wt% and 30.8 wt% recoveries of Mo and glass particles are obtained. Functional materials from this size fraction require further treatment since they attach on the whole surface of the EVA binder still laminated on glass.

Comminution by cutting mill can delaminate the solar panel, as the first stage recycling method, and expose the thin films containing critical metals, which are originally encapsulated in glass, and induce a selective liberation of functional materials in CIGS solar panel. Morphology analysis by observing the surface of broken particle using SEM-EDX demonstrates that the CIGS-Mo interface is dislodged after

milling. The mechanism of selective liberation is proposed. Cutting stress action due to milling reduces the size of glass and dislodges the adhesion between CIGS and Mo resulting in CIGS-EVA-glass particles and Mo-glass particles. A significant difference can be seen in the size fraction greater than 2360 μm where functional materials fully delaminated from molybdenum coated glass particles and particles with EVA binder on the surface are molybdenum free. The functional materials remains on EVA binder and results in the enrichment of metals in the coarse size fraction. Shearing induced by milling liberated some of the functional materials and reduced the size to less than 300 μm . Although the results suggest a selective liberation of functional material, 90 % of them are attached on EVA with glass and further treatment is required to de-coat the glass substrate and binder prior to subsequent chemical treatment. The morphology test shows that grinding can be a solution to polish the thin film materials containing critical metals. It suggests the size of grinding media is supposed to be less than 2360 μm so that the metals can be liberated while the generation of glass particles is not significant. The trial of a five minutes attrition scrubbing shows that grinding can be solution to de-coat the critical metals as the second stage recycling process. 86.26 w% of indium can be concentrated in 13.7 g fine particle with the concentration of 1506 ppm but it can be improved by adjusting the operating condition. The future work will focus on the liberation and concentration of photovoltaic material via grinding process with a suitable operating condition. It requires maximising the valuable materials, minimising the glass contained and yielding a suitable product for the last step metal refinery and extraction.

Equipment SPECIFICATIONS.

- Cutting mill (SM 200 smf, Retsch GmbH, Haan, Germany, serial No. 12102906103)
- Oven (NCD-120, NASER, Dongguan, China, serial No. YJ20180525002)
- Sieves (Laboratory Test Sieve, Endecotts Ltd, London, UK, serial No. 6118563, etc)
- Sieve shaker (Inclyno Sieve Shaker 3, Capco Test Equipment, Ipswich, UK, serial No.25431)
- Muffle furnace (CWF 12/23, Carbolite Ltd, Aston, UK, serial No. 21-401607)
- Centrifugal mill (ZM 200, Retsche GmbH, Haan, Germany, serial No. 1214040401P)
- Microwave digester (MARS 240/50, CEM Corporation, Matthews, USA, serial No. MD5420)
- ICP-MS (NexION 300X, KerklnElmer, Shelton, USA, serial No. 81XN2072303)
- SEM-EDX (FESEM, Cal Zeiss Microscopy Ltd, Cambridge, UK, serial No. sigma VP 02-77)
- Attrition scrubber (Fagergren Mineral Master, WEMCO, San Francisco, USA, serial No. 605400)

CRediT authorship contribution statement

Mingkai Li: Conceptualization, Methodology, Writing – original draft, Investigation. **Samuel D. Widijatmoko:** Conceptualization, Resources. **Zheng Wang:** Resources, Writing – review & editing. **Philipp Hall:** Supervision, Writing – review & editing, Project administration.

Declaration of Competing Interest

The authors declare that they have no known competing financial interests or personal relationships that could have appeared to influence the work reported in this paper.

Data availability

Data will be made available on request.

Acknowledgement

I would like to acknowledge the support from the Ningbo Municipal Key Laboratory on Clean Energy Conversion Technologies, the Zhejiang Provincial Key Laboratory for Carbonaceous Wastes Processing and Process Intensification Research funded by the Zhejiang Provincial Department of Science and Technology (2020E10018) as well as the Ningbo Science & Technology Innovation 2025 Major Project (2019B10050).

References

- [1] Hofmann M, et al. Critical raw materials: a perspective from the materials science community. *Sustain Mater Technol* 2018;17:e00074.
- [2] Grandell L, et al. Role of critical metals in the future markets of clean energy technologies. *Renew Energy* 2016;95:53–62.
- [3] Jones D. Global electricity review 2021:2021.
- [4] Xu Y, et al. Global status of recycling waste solar panels: a review. *Waste Manag* 2018;75:450–8.
- [5] Tao J, Yu S. Review on feasible recycling pathways and technologies of solar photovoltaic modules. *Sol Energy Mater Sol Cells* 2015;141:108–24.
- [6] Bakhiyya B, Labreche F, Zayed J. The photovoltaic industry on the path to a sustainable future—environmental and occupational health issues. *Environ Int* 2014;73:224–34.
- [7] SolarPower-Europe, *Global Market Outlook For Solar Power/2020–2024*, in *Solar Power Europe: Brussels, Belgium*. 2020.
- [8] IRENA, *Renewable Energy Statistics 2020*, T.I.R.E. Agency, Editor. 2020: Abu Dhabi.
- [9] IRENA, *Renewable Energy Statistics 2021*, T.I.R.E. Agency, Editor. 2021: Abu Dhabi.
- [10] Weckend S, Wade A, Heath G.A, *End of life management: solar photovoltaic panels*. 2016, National Renewable Energy Lab.(NREL), Golden, CO (United States).
- [11] Anttil A, Pthenakis V. Critical metals in strategic photovoltaic technologies: abundance versus recyclability. *Prog Photovolt Res Appl* 2013;21(6):1253–9.
- [12] Kazmerski LL. Solar photovoltaics R&D at the tipping point: a 2005 technology overview. *J Electron Spectrosc Relat Phenom* 2006;150(2–3):105–35.
- [13] Frisson, L., et al. *Recent improvements in industrial PV module recycling*, in *16th European Photovoltaic Solar Energy Conference*. 2000.
- [14] Chowdhury MS, et al. An overview of solar photovoltaic panels' end-of-life material recycling. *Energ Strat Rev* 2020;27:100431.
- [15] Padoan FCSM, Altimari P, Pagnanelli F. Recycling of end of life photovoltaic panels: a chemical prospective on process development. *Sol Energy* 2019;177:746–61.
- [16] Jackson P, et al. *Effects of heavy alkali elements in Cu(In, Ga)Se₂ solar cells with efficiencies up to 22.6%*. *physica status solidi (RRL) - Rapid Research Letters* 2016;10(8):583–6.
- [17] Miles RW, Zoppi G, Forbes I. Inorganic photovoltaic cells. *Mater Today* 2007;10(11):20–7.
- [18] Eron MN. Thin film CuInSe/sub 2//Cd (Zn) S heterojunction solar cell: characterization and modeling. Philadelphia, PA (USA): Drexel Univ; 1984.
- [19] European Commission, E., *Communication from the Commission to the European Parliament, the Council, the European Economic and Social Committee and the Committee of the Regions on the 2017 list of Critical Raw Materials for the EU*, in *COM (2017) 490 final*. 2017.
- [20] Alfantazi AM, Moskalyk R. Processing of indium: a review. *Miner Eng* 2003;16(8):687–94.
- [21] Hunt, A.J., *Element recovery and sustainability*. 2013: Royal Society of Chemistry.
- [22] Lokanc, M., R. Eggert, and M. Redlinger, *The availability of indium: the present, medium term, and long term*. 2015, National Renewable Energy Lab.(NREL), Golden, CO (United States).
- [23] Summaries, M.C., *US Geological Survey, Reston, VA 2022*. DOI: <https://doi.org/10.3133/mcs2022>, 2022.
- [24] McDonald NC, Pearce JM. Producer responsibility and recycling solar photovoltaic modules. *Energy Policy* 2010;38(11):7041–7.
- [25] Bang Y-Y, et al. Comparative assessment of solar photovoltaic panels based on metal-derived hazardous waste, resource depletion, and toxicity potentials. *Int J Green Energy* 2018;15(10):550–7.
- [26] Marwede M, et al. Recycling paths for thin-film chalcogenide photovoltaic waste – Current feasible processes. *Renew Energy* 2013;55:220–9.
- [27] Kushiya, K., Ohshita M, Tanaka M, *Development of recycling and reuse technologies for large-area Cu (InGa) Se/sub 2/-based thin-film modules*. in *3rd World Conference on Photovoltaic Energy Conversion, 2003. Proceedings of*. 2003. IEEE.
- [28] Campo, M.D., et al., *Process for recycling CdTe/Cds thin film solar cell modules*. 2003, Google Patents.
- [29] Widijatmoko SD, et al. Selective liberation in dry milled spent lithium-ion batteries. *Sustain Mater Technol* 2020;23:e00134.
- [30] Wills BA, Finch J. Wills' mineral processing technology: an introduction to the practical aspects of ore treatment and mineral recovery. Butterworth-Heinemann; 2015.
- [31] Wolf, J., *Recycling von Photovoltaik-Dünnschichtmodulen mit Hilfe eines Vakuum-Saugstrahlverfahrens*. 2009.
- [32] Krueger, L. *First solar's module collection and recycling program*. 2010 [cited 08.11.2022; Available from: http://www.solarscorecard.com/panel/pdf/Lisa_Krueger.pdf, zuletztgeprüftam.
- [33] Savvilitidou V, Gidaraks E. Pre-concentration and recovery of silver and indium from crystalline silicon and copper indium selenide photovoltaic panels. *J Clean Prod* 2020;250:119440.
- [34] Guldris Leon L, Hogmalm KJ, Bengtsson M. Understanding Mineral Liberation during Crushing Using Grade-by-Size Analysis—a Case Study of the Penuota Sn-Ta Mineralization, Spain. *Minerals* 2020;10(2):164.
- [35] Otsuki A, et al. Non-destructive characterization of mechanically processed waste printed circuit boards: X-ray fluorescence spectroscopy and prompt gamma activation analysis. *J Compos Sci* 2019;3(2):54.
- [36] Little L, et al. Using mineralogical and particle shape analysis to investigate enhanced mineral liberation through phase boundary fracture. *Powder Technol* 2016;301:794–804.
- [37] Bsi. *Bs 812–109: 1990 Testing aggregates., in Part 109: methods for determination of moisture content*. British Standard Institution; 1990.
- [38] Sharif S, et al. Thermal properties of ethyl vinyl acetate (EVA)/montmorillonite (MMT) nanocomposites for biomedical applications. *MATEC Web of Conferences* 2016:78.
- [39] Bsi. *Bs EN 62321–5: 2014 Determination of certain substances in electrotechnical products, in Part 5: Cadmium, lead and chromium in polymers and electronics and cadmium and lead in metals by AAS*. AFS, ICP-OES and ICP-MS. British Standard Institution; 2014.
- [40] Wills, B.A. Finch J.A, *Chapter 4-particle size analysis*. Wills' Mineral Processing Technology, 2016: p. 91-107.
- [41] Schubert G, Bernotat S. Comminution of non-brittle materials. *Int J Miner Process* 2004;74:S19–30.
- [42] LEIBNER, T., et al. *Method for evaluation of upgrading by liberation and separation*. in *XXVII International Mineral Processing Congress*. 2014.
- [43] Hesse M, Popov O, Lieberwirth H. Increasing efficiency by selective comminution. *Miner Eng* 2017;103:112–26.
- [44] Reichert M, et al. Research of iron ore grinding in a vertical-roller-mill. *Miner Eng* 2015;73:109–15.
- [45] Nishiwaki S, et al. MoSe 2 layer formation at Cu (In, Ga) Se 2/Mo Interfaces in High Efficiency Cu (In_{1-x}Ga_x) Se 2 Solar Cells. *Jpn J Appl Phys* 1998;37(1A):L71.
- [46] Hsiao K-J, et al. Electrical impact of MoSe 2 on CIGS thin-film solar cells. *PCCP* 2013;15(41):18174–8.
- [47] Colli A. The role of sodium in photovoltaic devices under high voltage stress: a holistic approach to understand unsolved aspects. *Renew Energy* 2013;60:162–8.
- [48] Harvey SP, et al. Sodium accumulation at potential-induced degradation shunted areas in polycrystalline silicon modules. *IEEE J Photovoltaics* 2016;6(6):1440–5.
- [49] Little L, et al. Fine grinding: How mill type affects particle shape characteristics and mineral liberation. *Miner Eng* 2017;111:148–57.